

# *Development of a prototype real-time sting-jet precursor tool for forecasters*

Article

Published Version

Creative Commons: Attribution 4.0 (CC-BY)

Open access

Gray, S. L. ORCID: <https://orcid.org/0000-0001-8658-362X>,  
Martinez-Alvarado, O. ORCID: <https://orcid.org/0000-0002-5285-0379>, Ackerley, D. and Suri, D. (2021) Development of a  
prototype real-time sting-jet precursor tool for forecasters.  
Weather, 76 (11). pp. 369-373. ISSN 1477-8696 doi:  
<https://doi.org/10.1002/wea.3889> Available at  
<https://centaur.reading.ac.uk/94616/>

It is advisable to refer to the publisher's version if you intend to cite from the work. See [Guidance on citing](#).

To link to this article DOI: <http://dx.doi.org/10.1002/wea.3889>

Publisher: Wiley

All outputs in CentAUR are protected by Intellectual Property Rights law, including copyright law. Copyright and IPR is retained by the creators or other copyright holders. Terms and conditions for use of this material are defined in the [End User Agreement](#).

[www.reading.ac.uk/centaur](http://www.reading.ac.uk/centaur)

**CentAUR**

Central Archive at the University of Reading

Reading's research outputs online

# Development of a prototype real-time sting-jet precursor tool for forecasters

Suzanne L. Gray<sup>1</sup> ,  
Oscar Martínez-Alvarado<sup>2</sup> ,  
Duncan Ackerley<sup>3</sup>  and  
Dan Suri<sup>3</sup>

<sup>1</sup>Department of Meteorology, University of Reading, UK

<sup>2</sup>National Centre for Atmospheric Science, and Department of Meteorology, University of Reading, UK

<sup>3</sup>Met Office, Exeter, UK

Damaging surface winds in some European storms have been attributed to descending mesoscale airstreams termed sting jets. The development of a prototype real-time tool that Met Office forecasters can use to identify favourable conditions for sting jet occurrence in extratropical cyclones is presented. The motivation is to improve national severe weather warnings. We have previously developed a convective-instability-based tool to identify sting-jet precursors for research purposes and applied it to storms in reanalyses and climate models with insufficient spatial resolution to represent sting jets. Here we describe the challenges of applying this research-derived diagnostic to output from an operational forecast system and demonstrate its usefulness for a recent winter storm. Through close collaboration with the researchers and forecasters from the Met Office, the diagnostic has been adapted to work on output from the Met Office's operational global ensemble forecasts as it becomes available. Since autumn 2019, forecasters have been able to view graphical output informing them whether storms impacting the UK and Europe (up to 7 days in the future) have the precursor. The tool has already proven useful in informing guidance for severe weather warnings, including those issued by the Met Office's impact-based National Severe Weather Warning Service that goes out to seven days ahead and is the primary hazardous weather warning service for the public and emergency responders.

## Sting jets in extratropical cyclones

Extratropical cyclones are a major cause of hazardous weather, mainly due to intense or sustained wind, rainfall or snowfall. An extreme windstorms catalogue (Roberts *et al.*, 2014) lists the insured losses for the most devastating recent storms, as identified by insurance experts from Willis Re. The Great Storm of October 1987, the first windstorm in which a sting jet was formally identified (Browning, 2004), is the second most costly of these with an insured loss of \$6.3bn (indexed to 2012 values). Strong surface winds in extratropical cyclones typically arise from the two synoptic-scale low-level wind jets associated with the so-called warm conveyor belt (WCB) that ascends ahead of the cold front, and the cold conveyor belt (CCB) that wraps rearwards around the cyclone (Figure 1). In some cyclones, a transient (timescale  $\sim$  several hours), smaller-scale (surface footprints typically  $<100$ km wide) feature termed a sting jet also occurs (e.g. Schultz and Browning (2017)). Sting jets can lead to strong surface winds and gusts in the dry air ahead of the convex 'cloud

head' seen in satellite images of extreme cyclones, such as that visible in the upper-left quadrant of Figure 3(b).

Sting jets have been formally studied in more than 10 cyclones affecting Europe (table 2 of the review by Clark and Gray (2018)), and are suspected to have occurred in many more. Distinctive cloud features visible in satellite imagery of cyclones can indicate a sting jet, but this identification is only possible once the cyclone is at the stage when sting jets are about to occur or actually occurring. At longer lead times, Met Office forecasters subjectively consider upper-tropospheric trough and jet-stream configurations and their potential to lead to Shapiro–Keyser-type cyclogenesis (Shapiro and Keyser, 1990), as well as high-resolution convection-permitting model output,<sup>1</sup> in considering sting-jet threat. A challenge to forecasters is that operational global forecast models are currently borderline in their ability to resolve sting jets, in contrast to the

<sup>1</sup>5-day convection-permitting forecasts from the Met Office's UK variable resolution (UKV) model are available twice-daily.

## Conditional symmetric instability (CSI)

CSI release occurs when an air parcel becomes saturated in an environment that is stable to vertical and horizontal displacement (i.e. gravitationally and inertially stable, respectively) but not to slantwise displacement. If gravitational or inertial instability are present, they will be released preferentially to slantwise instability. CSI release leads to slantwise motions. CSI can be considered as equivalent to the conditional instability that leads to the familiar upright convection upon release but evaluated along sloping surfaces of geostrophic absolute momentum instead of vertically. It exists where surfaces of geostrophic absolute momentum slope less steeply in the vertical than surfaces of saturated equivalent potential temperature, a situation that is common in baroclinic zones such as fronts (Glinton *et al.*, 2017).

The energy available from CSI release can be quantified using slantwise convective available potential energy (slantwise CAPE). CAPE is the maximum kinetic energy available to an air parcel for (upright) convection due to latent heating from condensation. Slantwise CAPE (SCAPE) is equivalent to CAPE diagnosed along slanting surfaces of geostrophic absolute momentum. Finally, downdraught SCAPE (DSCAPE) is the maximum kinetic energy available to an air parcel descending along such momentum surfaces due to latent cooling from the evaporation of precipitation that is just sufficient to keep the air parcel saturated. For further explanation of CSI, please see Schultz and Schumacher (1999) or Clark and Gray (2018).

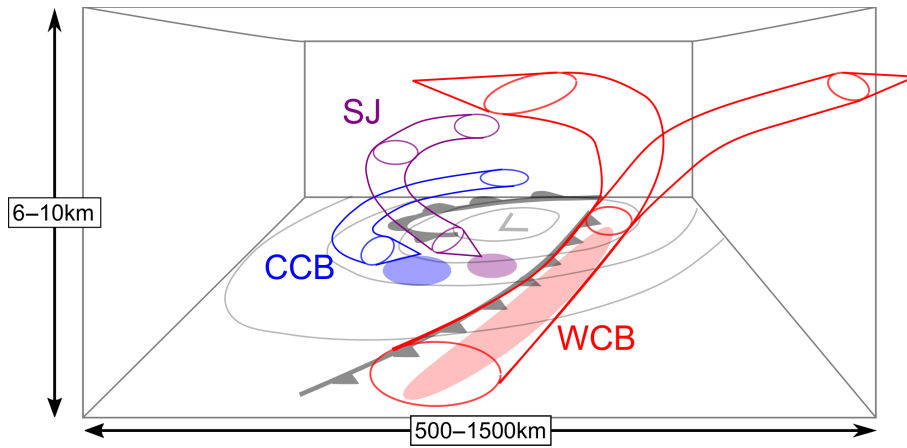


Figure 1. Conceptual model of the 3D structure of a Shapiro–Keyser cyclone showing the WCB (red), CCB (blue) and sting jet (magenta). For each jet, the region of strong surface winds is indicated by the shaded ellipse. (Source: Clark and Gray, 2018.)

CCB and WCB jets that are well resolved. Furthermore, the coarser resolution of ensemble operational global forecasts, used for probabilistic forecasts of hazards, is not sufficient to represent sting jets at all. This limits the ability of forecasters to predict, at several days lead time, whether a cyclone is likely to develop a sting jet. Here we describe the development of a prototype real-time tool that Met Office forecasters can use to identify favourable conditions for sting jet occurrence in these ensemble forecasts.

## From research diagnostic tool to operational implementation

Model horizontal grid spacings of 10–15 km or less are needed to resolve sting jets because they are associated with the release of mesoscale instabilities, such as conditional symmetric instability (CSI, see text box), that are only released for sufficiently high resolutions. The shallow scale of the descending sting jet also provides a constraint on vertical grid spacing of about 240 m in the mid-troposphere for a 12 km horizontal grid spacing (Clark and Gray, 2018). While high-resolution (convection-permitting) limited domain operational weather forecast models easily meet these resolution requirements, the global models needed for longer-range forecasts struggle or fail. While the resolution of the Met Office operational global deterministic model is borderline for resolving sting jets (10 km horizontal grid spacing and 275–350 m vertical level spacing<sup>2</sup>), the global configuration of the operational ensemble (known as MOGREPS-G) is too coarse (20 km horizontal grid spacing and the same vertical level set). The presence of a sting jet can only be confirmed in sting-jet resolving model output by calculating back trajectories from a possible sting-jet wind maximum. Only then

can it be determined whether the air has sting-jet characteristics and has descended from the cloud head tip.

The failure of global ensemble weather forecast, reanalysis and climate models to resolve sting jets indicates that determining their climatological characteristics is not as simple as diagnosing them in model or reanalysis output. Instead, we have developed an innovative and skilful method to diagnose those cyclones that have a precursor for, and so are likely to produce, sting jets (Martínez-Alvarado *et al.*, 2013). There are several mechanisms attributed to sting jet formation, as synthesised in figure 8 of Clark and Gray (2018). However, the strongest sting jets have typically been associated with the release of mesoscale instabilities such as CSI. The sting-jet precursor diagnostic identifies cyclones that are likely to produce sting jets by assessing the presence of this type of convective instability in an analogous way to the diagnosis of large values convective available potential energy (CAPE) as a precursor for thunderstorm development. We quantify the CSI that can be released by downdraughts by calculating downdraught slantwise CAPE (DSCAPE, see text box).

The precursor diagnostic described above has previously been applied to multidecadal ECMWF ERA-Interim reanalysis (ERA-I) data and climate model output. About a third of North Atlantic cyclones from ERA-I were found to have the precursor (indicating that sting jets are likely to have occurred in these cyclones) with a higher proportion for explosively deepening cyclones (Martínez-Alvarado *et al.*, 2012; Hart *et al.*, 2017). The wind risk, diagnosed from ERA-I and the climate model output, associated with sting-jet precursor cyclones in the current climate was enhanced compared to cyclones without a precursor even though sting jets are not resolved in the models or the reanalysis. This enhancement likely occurs because cyclones with the precursor tend to be rap-

idly developing cyclones associated with strong frontal gradients and severe CCB winds. In reality, the sting jet would further increase these wind speeds and change the location of the strongest winds. Hence, the precursor provides a warning flag for damaging winds irrespective of whether a sting jet actually occurs.

Here we describe the implementation of a prototype software tool, based on the sting-jet precursor diagnostic, running in near-real time on output from the operational MOGREPS-G system and providing forecasters with graphical outputs. The MOGREPS-G ensemble is used as it provides probabilistic information from 36 equally probable forecasts created by combining two, time-lagged, 18-member ensembles. The composition of the project team, two university researchers who led the development of the precursor diagnostic and a researcher and forecaster (a Chief Operational Meteorologist) both from the Met Office, was key to the project success. The challenges involved (algorithm speedup, algorithm implementation and engagement with forecasters) are now described.

## Algorithm speedup

The algorithm to detect sting-jet precursors in model output follows Martínez-Alvarado *et al.* (2012) and comprises three major steps: (1) tracking extratropical cyclones, (2) extracting meteorological fields around tracked cyclone centres and re-gridding them onto a rotated grid, centred around the cyclone centres, with a grid spacing of  $0.5^\circ \times 0.5^\circ$  and (3) computing sting-jet precursors. Cyclones with sufficient DSCAPE in the cloud head are diagnosed as having a sting-jet precursor. The bottleneck is the calculation of DSCAPE in the third step where atmospheric soundings along slantwise, descending surfaces of constant absolute momentum are calculated. To speed up the calculation for operational implementation, we adapted an estimated formula that uses vertical atmospheric soundings to derive SCAPE (as used in the CSI climatology by Chen *et al.* (2018)) in order to calculate DSCAPE. Comparison of precursor regions calculated using the slantwise and vertical calculations found greater DSCAPE magnitudes from the vertical calculations, leading to an increased likelihood of sting-jet precursor diagnosis, but very similar spatial patterns, i.e. DSCAPE was diagnosed in the same regions of the tested cyclones. The vertical-calculation method was used to predict sting-jet precursors diagnosed using the slantwise-calculation method for 130 cyclones from 9 months of climate model data. This prediction yielded hit and false alarm rates of 0.925 and 0.312, respectively, demonstrating that the two methods are acceptably consistent in their identification of the precursor.

<sup>2</sup>For a mid-latitude grid point at 3–5 km above sea level.



## Algorithm implementation

Porting the code from the University of Reading system, where it had been developed, to the Met Office required the following steps. First, translation of parts of the code from MATLAB to Python. Second, ensuring consistency between the versions and features of the tracking algorithm (TRACK developed by Hodges (1994)) between the University of Reading and Met Office versions. Third, enhancement of the model output fields to include all fields required for the diagnostic: horizontal wind components, potential temperature, specific humidity and non-dimensional (Exner) pressure on model levels, as well as orography, mean sea-level pressure and 850hPa relative vorticity pre-smoothed to T42 resolution (i.e. truncated to total wavenumber 42, about 310km resolution at the equator) which is required as an input to the tracking algorithm. Fourth, implementation of scripts to move the required outputs from the operational forecasts to a separate location for processing as soon as they are available (typically 10–14 hours after the forecast is initiated) and before they are automatically deleted (about 24 hours after generation). Finally, automation of the sequence of steps described above. This porting was only possible through close collaboration and iterative problem solving between the Met Office and University of Reading researchers and currently, at the time of writing, the algorithm runs on the 18-member MOGREPS-G ensembles initiated daily at 0000 and 1200 UTC.

## Engagement with forecasters

Met Office forecasters routinely look at various model outputs from both the Met Office and other operational centres to inform their weather guidance, including, for example, diagnosed cyclone tracks from ensembles, in addition to the direct model outputs. Chief Met Office Operational Meteorologist (and co-author) Dan Suri was involved in the development of the proposal that funded this work and introduced the other Chief and Deputy Chief Met Office Operational Meteorologists to the new sting-jet precursor diagnostic. The graphical outputs show cyclone tracks and ensemble sting-jet precursor probability in two ways: (i) over the entire forecast (akin to the strike probabilities often presented for tropical cyclone forecasts) and (ii) as snapshots available throughout each forecast (both for a given forecast base time). The example in Figure 2 shows snapshots of both the ensemble-based probabilities of the presence of the sting-jet precursor (Figure 2(a)) and the precursor in individual members (Figure 2(b)). The plots are accessed via an internal Met Office web page, and the domain and map projection were selected to be consistent with other images rou-

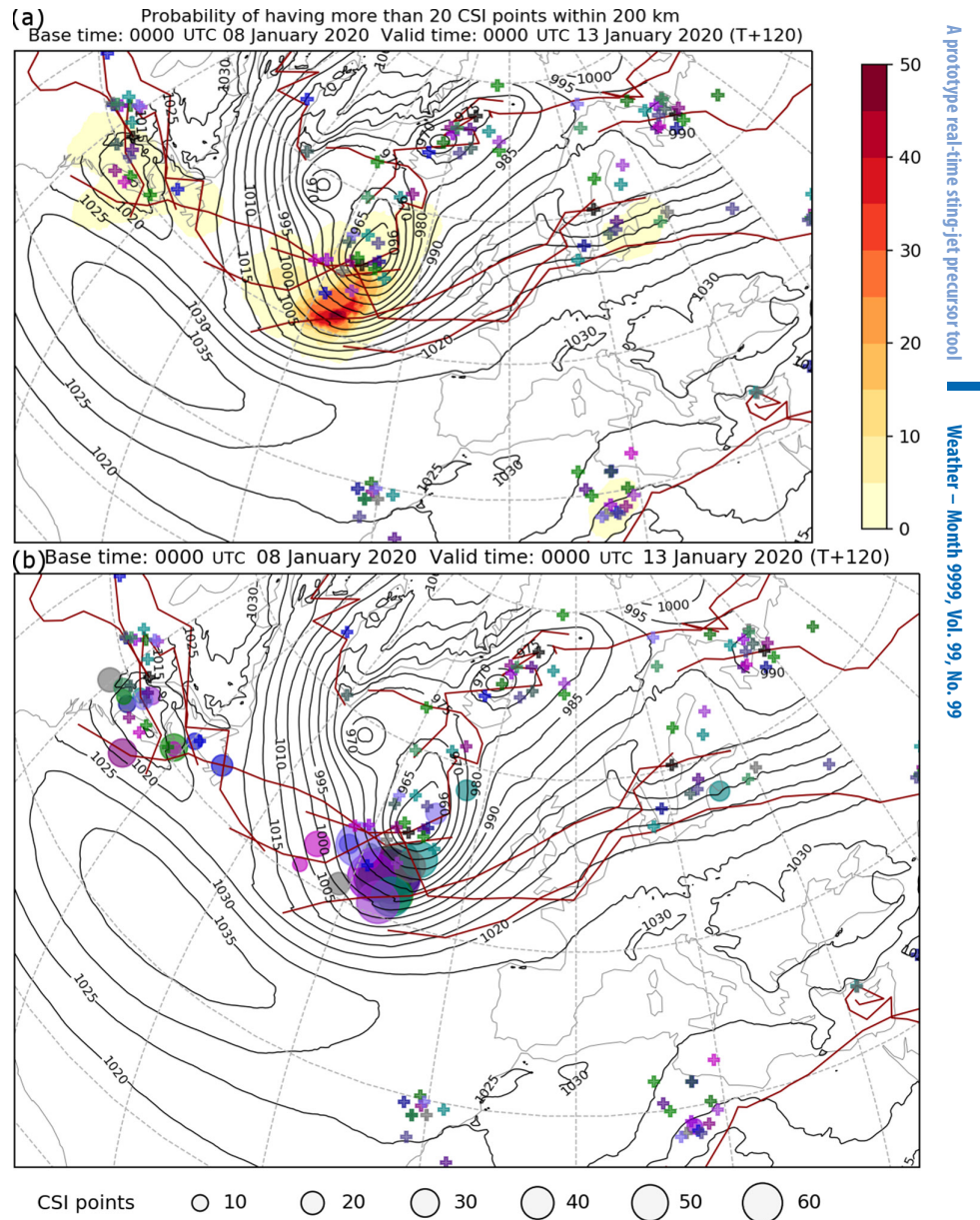


Figure 2. Sample graphical sting-jet precursor output for forecasters: 5-day forecast valid at 0000 UTC 13 January 2020. (a) Ensemble-based probability of sting-jet precursor for greater than 20 CSI points (on a  $0.5^\circ \times 0.5^\circ$  grid) within 200km (shaded). The CSI points are all within 1000km of a cyclone centre and constitute sets whose centroids are within 700km of a cyclone centre in the cloud head sector and with moisture available for the instability to be released. (b) Locations of the centroids of sets of CSI points (coloured circles); the sizes of the circles are proportional to the number of points in the set (10–60 grid points within 200km of each centroid). Overlain on both plots are the cyclone tracks of all the storms identified during the period (dark red lines) and the mean sea-level pressure (black contours every 5hPa) at the verification time from the control ensemble member. The plus symbols along the tracks indicate the locations of the cyclone centres at the verification time colour-coded by ensemble member (with matching colours for the CSI centroids in (b)).

tinely used by the forecasters. Users can flip between different forecast base times and snapshot times and can choose the minimum size (in  $0.5^\circ \times 0.5^\circ$  boxes) of the region required to meet the precursor instability criteria (20, 30 or 40 grid points within 200km from each location on the map). Forecasters can use the graphical outputs to objectively assess the potential for winds to be stronger than the model predicts due to a sting jet. They can then use this assessment alongside

other diagnostics and some sense of calibration after experiencing multiple events. This approach contrasts with the subjective assessment based on the likelihood of Shapiro–Keyser cyclogenesis used previously.

## Case example: Storm Brendan

Several cyclones impacting the United Kingdom have been flagged by the precursor diagnostic since its routine implementa-

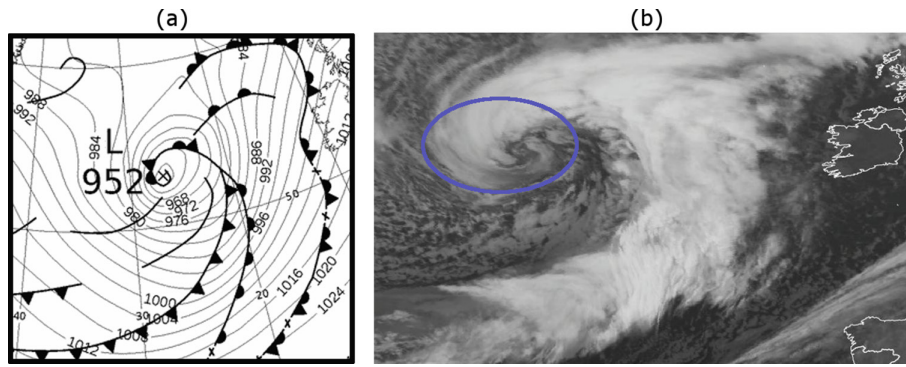


Figure 3. (a) Met Office analysis chart and (b) infra-red satellite imagery at 0000 UTC 13 January 2020 with region of cloud banding indicated by the ellipse. Analysis chart is Crown copyright; satellite imagery is from EUMETSAT (2020).

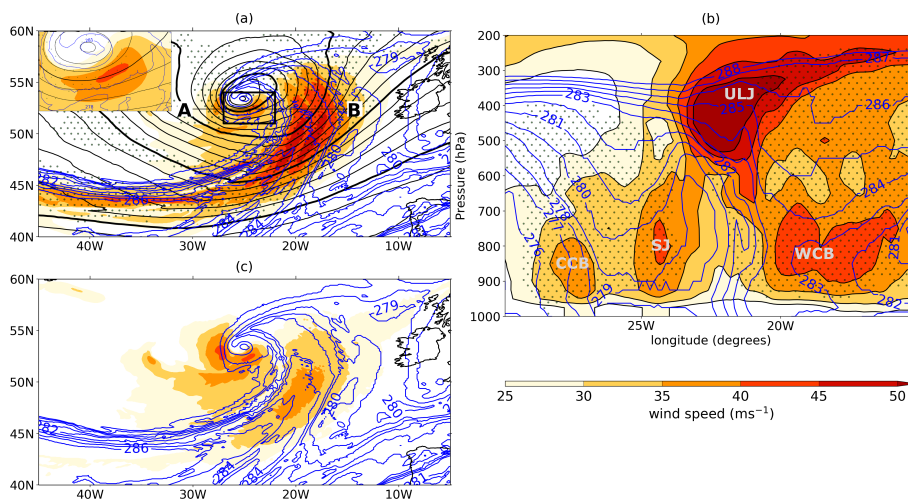


Figure 4. Sting-jet diagnosis from 18-hour operational deterministic model forecast valid at 0100 UTC 13 January 2020: (a) map of 800hPa horizontal wind speed (colour), selected 800hPa wet-bulb potential temperature contours (blue), 700hPa relative humidity (stippled exceeding 90%) and mean sea-level pressure (black contours every 4hPa with 960, 980, 1000 and 1020hPa contours thickened), insert shows a zoom of the region within the black box; (b) vertical cross-section between A and B marked in (a) and connected by a thin line (30–15°W at 52.4°N) showing the same fields (except mean sea-level pressure) and with jets labelled; (c) 10m wind gusts with 800hPa wet-bulb potential temperature (as in (a)). The black box in (a) encloses the sting jet and frontal fracture region and is the region from which back trajectories were calculated, and the colour bar applies to all three panels.

tion. Here we illustrate the behaviour of the diagnostic in a single case; detailed analysis of the characteristics of the precursor and its association with extreme surface winds and gusts is left to a future study. Although observational evidence for sting jets over the ocean is usually limited to indicative cloud features in satellite imagery and, when available, near-surface winds from scatterometers, short-range sting-jet resolving model forecasts can also be used to determine whether a sting jet occurred in a cyclone. Strong winds associated with Storm Brendan affected the United Kingdom on 13 January 2020. As Brendan approached northwest Scotland and then turned northwards towards southern Iceland, the Met Office issued a yellow wind warning for northwestern parts of the United Kingdom.

The strongest low-level gusts were over northern and western Scotland and often exceeded 60kn (with a maximum of 76kn at South Uist (Kendon, 2020)), causing disruption to transport and power supplies. Storm Brendan deepened explosively as it crossed the North Atlantic with a 24-hour central mean sea-level pressure drop of 49hPa from 997hPa at 0600 UTC 12 January to 948hPa at 0600 UTC 13 January (according to Met Office analyses). Cloud banding is visible within the tip of the cloud head that lies along the analysed bent-back front at 0000 UTC on 13 January (Figure 3) and was even more clearly evident at 2100 UTC on 12 January (not shown). Although analysed according to the Norwegian conceptual cyclone model, a frontal fracture region is evident in the forecast wet-bulb potential temperature

field at this time (within the black box in Figure 4(a)). This fracture and the further deepening of the storm indicate that the cyclone is in stage III of evolution according to the Shapiro–Keyser conceptual model (Shapiro and Keyser, 1990), the stage when sting jets typically occur.

Aided by longer-lead time forecast output, Met Office internal guidance signalled the potential for a deep, impactful wind-storm to affect the British Isles 6 or 7 days in advance. Even at a lead time of 5 days, the ensemble-based diagnostic indicated greater than 30% probability of a sting-jet precursor existing to the southwest of the cyclone centre (i.e. in the tip of the cloud head) at 0000 UTC 13 January (Figure 2(a)). This high probability is a consequence of strong agreement among the ensemble members in the position of Storm Brendan and the location of its associated precursor region (Figure 2(b)). The precursor reveals suitable antecedent conditions for sting jets in the 5-day forecast valid at this time. Analysis of the 67 equivalent images available for 5-day forecasts from December 2019–February 2020 reveals similar coherent regions exceeding 30% probability near marine cyclone centres within a North Atlantic–European domain on 8 additional days (relating to six cyclones). Hence, such high probabilities occur relatively infrequently.

Some evidence for the existence of a sting jet in reality comes from short-range operational deterministic model output: unlike the ensemble model configuration, the resolution of the deterministic configuration is borderline for resolving sting jets. The 800hPa wind speed reveals a small, localised region of enhanced strength in the frontal fracture region to the south of the cyclone centre (in the box marked in Figure 4(a)). This region is distinct from the WCB jet found ahead of the cold front and two other small regions of enhanced winds found in the colder air to the south and southwest of the enhanced frontal fracture winds. A short-range forecast has been analysed so that back trajectories can be calculated. Back trajectories (not shown) from the marked region indicate a coherent set of trajectories that descend by about 100hPa over 6 hours while accelerating, drying slightly and conserving wet-bulb potential temperature until the final 2 hours: these trajectories are consistent with a weak sting jet. A cross-section through the storm (Figure 4(b)) reveals four distinct wind jets: three lower-tropospheric jets consistent with the CCB, a sting jet (SJ: in the frontal fracture region with weak wet-bulb potential temperature gradients) and the WCB, and one upper-tropospheric jet (ULJ) centred at about 400hPa. While the CCB and WCB jets are entirely in cloud (indicated by the stippling), the sting jet lies partially in the dry air in the dry slot region



of the cyclone. The sting-jet core exceeding  $40\text{ms}^{-1}$  is at about 800hPa, but strong winds extend towards the surface and are associated with enhanced surface wind gusts that exceed those associated with the WCB (Figure 4(c)). Satellite-derived winds (from the Advanced Scatterometer, ASCAT, on the EUMETSAT METOP satellite, not shown) are consistent with the model forecast, with surface winds exceeding 55kn ( $\sim 28\text{ms}^{-1}$ ) directly south of the cyclone centre in the swath available from a few hours prior to the time shown in Figure 4; however, the CCB and SJ cannot be distinguished in these observations. The sting jet in Storm Brendan no longer existed when the storm affected the United Kingdom. However, although the sting jet was not the cause of the damage in the United Kingdom, the precursor diagnostic warned forecasters that a storm with strong winds including a possible sting jet could be approaching the United Kingdom 5 days ahead. This storm also demonstrated proof of concept in a storm season which, although active, did not have many storms with sting-jet potential.

## Outlook

The behaviour and usefulness to forecasters of the sting-jet precursor diagnostic, and the way in which the output is presented, needs to be evaluated over a period including several high impact storms. Of particular use will be forecaster evaluation of the most appropriate size to consider for the sting-jet precursor region. Once this evaluation and calibration stage has been completed, this diagnostic will be refined and remain available to the Met Office forecasting community for whom it will provide an objective method of identifying additional details of potentially damaging windstorms, especially in the medium-range forecast period. This will aid a number of Met Office forecasting efforts such as wind warnings across multiple customer groups, including the National Severe

Weather Warning Service (Neal *et al.*, 2014) and cross-organisational initiatives such as European storm naming. The data generated are also a potential resource for future research as some diagnostics are being permanently saved at the Met Office.

## Acknowledgements

The authors gratefully acknowledge the assistance provided by Kevin Hodges (University of Reading) on the use of his cyclone tracking algorithm and Simon Thompson (Met Office) for implementing the additional output fields required in the operational MOGREPS-G output. Code to calculate DSCAPE from vertical profiles is available from github at <https://github.com/omartineza/csisounding>. Precursor tool outputs and the operational global forecast outputs used are archived at the Met Office. Please contact the authors for details.

SLG and OM-A were funded by the NERC (Natural Environment Research Council) UK Climate Resilience programme (grant reference NE/S016384/1). DA is supported by the Joint BEIS/Defra Met Office Hadley Centre Climate Programme (GA01101).

## References

- Browning KA.** 2004. The sting at the end of the tail: damaging winds associated with extratropical cyclones. *Q. J. R. Meteorol. Soc.* **130**: 375–399.
- Chen T-C, Yau MK, Kirshbaum DJ.** 2018. Assessment of conditional symmetric instability from global reanalysis data. *J. Atmos. Sci.* **75**: 2425–2443.
- Clark PA, Gray SL.** 2018. Sting jets in extratropical cyclones: a review. *Q. J. R. Meteorol. Soc.* **144**: 943–969.
- Glinton MR, Gray SL, Chagnon JM *et al.*** 2017. Modulation of precipitation by conditional symmetric instability release. *Atmos. Res.* **185**: 186–201.
- Hart NCG, Gray SL, Clark PA.** 2017. Sting-jet windstorms over the North Atlantic: climatology and contribution to extreme wind risk. *J. Clim.* **30**: 5455–5471.

**Hodges KI.** 1994. A general method for tracking analysis and its application to meteorological data. *Mon. Weather Rev.* **122**: 2573–2586.

**Kendon, M.** 2020. *Storms Atiyah (December 2019) and Brendan (January 2020)*. [https://www.metoffice.gov.uk/binaries/content/assets/metofficegovuk/pdf/weather/learn-about/uk-past-events/interesting/2020/2020\\_01\\_storm\\_brendan.pdf](https://www.metoffice.gov.uk/binaries/content/assets/metofficegovuk/pdf/weather/learn-about/uk-past-events/interesting/2020/2020_01_storm_brendan.pdf).

**Martínez-Alvarado O, Gray SL, Catto JL *et al.*** 2012. Sting jets in intense winter North-Atlantic windstorms. *Environ. Res. Lett.* **7**: 024014

**Martínez-Alvarado O, Gray SL, Clark PA *et al.*** 2013. Objective detection of sting jets in low-resolution datasets. *Meteorol. Appl.* **20**: 41–55.

**Neal RA, Boyle P, Grahame N *et al.*** 2014. Ensemble based first guess support towards a risk-based severe weather warning service. *Meteorol. Appl.* **21**: 563–577.

**Roberts JF, Champion AJ, Dawkins LC *et al.*** 2014. The XWS open access catalogue of extreme European windstorms from 1979 to 2012. *Nat. Hazards Earth Syst. Sci.* **14**: 2487–2501.

**Schultz DM, Browning KA.** 2017. What is a sting jet? *Weather* **72**: 63–66.

**Schultz DM, Schumacher PN.** 1999. The use and misuse of conditional symmetric instability. *Mon. Weather Rev.* **127**: 2709–2732.

**Shapiro MA, Keyser D.** 1990. Fronts, jet streams and the tropopause, in *Extratropical Cyclones*. Newton CW, Holopainen EO (eds). American Meteorological Society: Boston, MA, pp 167–191.

Correspondence to: S. L. Gray

[s.l.gray@reading.ac.uk](mailto:s.l.gray@reading.ac.uk)

© 2020 The Authors. *Weather* published by John Wiley & Sons Ltd on behalf of the Royal Meteorological Society

This is an open access article under the terms of the Creative Commons Attribution License, which permits use, distribution and reproduction in any medium, provided the original work is properly cited.

doi: 10.1002/wea.3889